Lifescience Global

Journal of Coating Science and Technology
http://www.lifesciencesglobal.com/journals/journal-of-coating-science-and-technology

Characteristics of CVD Grown Diamond Films on Langasite Substrates

Awadesh Kumar Mallik[1,3,*], Snigdha Roy[1], Vamsi Krishna Balla[1], Sandip Bysakh[1] and Radhaballabh Bhar[2]

[1]*CSIR – Central Glass & Ceramic Research Institute, Kolkata 700032, West Bengal, India*

[2]*Department of Instrumentation Science, Jadavpur University, Kolkata 700032, West Bengal, India*

[3]*Hasselt University, Institute for Materials Research (IMO) and IMEC vzw, IMOMEC, Diepenbeek, Belgium*

Abstract: Surface acoustic wave (SAW) devices consist of a piezoelectric substrate with interdigitated (IDT) electrodes. These devices can be used to fabricate wireless and passive sensors that can be mounted in remote and/or inaccessible places. If encapsulated with CVD diamond, the SAW devices can be made to operate under extremely hostile conditions. The piezoelectric layer (AlN, ZnO etc.) deposited on the diamond or an inverse system can increase the frequency of the SAW device. Most piezoelectric materials (such as quartz) show phase transition temperatures below diamond deposition temperature (650°-1100ºC), preventing their use as a substrate for diamond growth. Langasite $La_3Ga_5SiO_{14}$ (LGS) is recently fabricated piezoelectric material that can withstand high temperatures without being deteriorated. LGS does not have phase transitions up to its melting point of 1470 °C.

Here we report the deposition of diamond films by microwave plasma CVD in methane-hydrogen gas mixtures on polished and rough surfaces of the LGS substrates seeded with nanodiamonds. No buffer layer between the substrate and the coating had been used. The effect of substrate pretreatment (PT) was also investigated on the growth behaviour of diamond films on LGS. The resulting films are characterised by Raman spectroscopy, X-ray diffraction (XRD), field-emission scanning electron microscopy (FESEM), X-ray photoelectron spectroscopy (XPS). The effect of substrate roughness on the growth behaviour was found to favour bigger grain sizes on the unpolished substrates. Whereas, the effect of substrate pretreatment (PT) was found to produce unique microstructural features with better polycrystalline diamond (PCD) quality than on the substrates without PT. Raman signals confirm the deposition of PCD in all the cases but the X-ray results interestingly show new phase formation of hcp and rhombohedral diamond lattice structures under CVD growth environment.

Received on 29-10-2019
Accepted on 13-11-2019
Published on 08-01-2020

Keywords: Microwave plasma CVD, polycrystalline diamond, langasite, SAW.

DOI: https://doi.org/10.6000/2369-3355.2019.06.02.2

1. INTRODUCTION

For the past few years, the automotive industry has witnessed a large increase in electronic instrumentation aboard the vehicles. In particular, cylinder-pressure measurements at the combustion engines has become a standard instrument in engine research and development, as well as in production quality assurance [1]. The Surface Acoustic Wave (SAW) technology provides an excellent means to fabricate temperature and pressure sensors [2] that can be assembled in combustion engines, for monitoring cylinder pressure or temperature at critical spots. In fact, SAW devices are passive components with Interdigitated Transducer (IDT) metal lines patterned on a piezoelectric substrate, which can be remotely interrogated by means of an RF beam (eliminating the need of wiring) and don't require external power or batteries (thus eliminating the need of wiring). On the other side, RFID (Radio-Frequency Identification) is an automatic wireless identification method where a proper read-out unit sends an RF pulse over an object and interprets the pulse reflected by the tag attached to it. By coupling RFID and SAW sensors (simply by patterning a series of reflectors on the piezoelectric material surface), a series of wireless sensors can be interrogated by the same unit [3]. This efficient and technological simple sensor system used inside automotive engines can also be extended to underground petroleum pipelines for continuous remote monitoring, in real-time, of the temperature and/or pressure in specific places inside, inaccessible by more

*CSIR – Central Glass & Ceramic Research Institute, Kolkata 700032, West Bengal, India; E-mail: amallik@cgcri.res.in, awadesh.mallik@gmail.com

conventional measuring devices involving wires. This system is also of great interest to other industrial segments such as aerospace, nuclear power, gas and petroleum exploration, industrial process control, telecommunications and power electronics.

The goal of this work is to develop an encapsulation material [4-6] – i.e. polycrystalline diamond (PCD) coating, for SAW-based sensors that can operate under the extreme environmental conditions typical of combustion engines or of petroleum underground pipelines and its explorations (temperatures up to 400°C and accelerations up to 2000 g). The SAW devices are fabricated by patterning IDTs and reflection electrodes on high-temperature piezoelectric materials like langasite (LGS, $La_3Ga_5SiO_{14}$) and lithium niobate ($LiNbO_3$). These materials have already been used to fabricate high-temperature SAW sensors [1,7-10]. The devices can be assembled with an RF antenna on a proper substrate and the whole set can be coated with diamond. Diamond gathers some properties that make it the best encapsulation material: it is hard and chemically inert, it is electrically insulating but thermally conductor and it is intrinsically resistant to wear. Besides, the versatility of Chemical Vapour Deposition (CVD) allows the deposition of diamond in the form of thin conformal films. PCD coating on such piezoelectric sensor materials will protect them from extreme environments of temperature, pressure, wear and corrosion. Special attention will be given to the CVD diamond seeding procedure, an essential step to assure the deposition of diamond in the form of thin conformal films and to decrease the wave scattering and the propagation losses at the interface. In particular, the new nucleation process (NNP) [11], will be complemented by the use of nanodiamond seeding and/or seeding slurries [12].

Change in semiconductor resistivity with strain i.e. piezoresistivity property of p-type NCD coatings [13] on SiO_2/Si substrates was found to perform well at high temperatures (500^{o}C) where conventional silicon-on-insulator (SOI) piezoresistor fails [14]. Single crystalline diamond and polycrystalline diamond films [15-17] show a high gauge factor (change in resistivity per unit strain) in the range of 500–4000 and 10–100, respectively, compared to diamond-like carbon (DLC) films 36–1200 [18]. On the other hand, the diamond is not piezoelectric.

Frequency of SAW device is the ratio of sound velocity divided by interdigitated spacing/wavelength. IDT spacing is limited by the lithographic technique but one way of increasing the SAW frequency is to use material with high phase velocity. Diamond is not only the best acoustic propagator but also it has the highest thermal conductivity, which ensures high thermal stability of the SAW device parameters [19]. Al/ZnO/Diamond layered structure was fabricated for testing phase velocity and coupling co-efficient (K2: effective conversion of RF signal into the surface acoustic wave and vice versa) of propagating sound wave at 2.45 GHz frequency. Although, diamond is not piezoelectric, but it has the highest elastic modulus and sound velocity, which make it an ideal substrate for SAW devices [20]. AlN (hexagonal) has a higher phase velocity than ZnO. So AlN/NCD/Si SAW device was also tried to minimise velocity dispersion, thus increasing the coupling coefficient. Benedic *et al*. could achieve 9472m/s phase velocity with 18.9μm thick NCD, 4μm thick AlN layered structure and 32μm aluminium IDT spacing or λ [21]. This same group tried out ZnO/Diamond layered structure with 32 μm wavelength, 3 μm ZnO and 25 μm diamond first layer thickness and reported acoustic phase velocity 9696 m/s, electromechanical coupling coefficient: $K2$=0.75%, temperature coefficient of frequency: TCF=29 ppm/^{o}C [22]. They theoretically calculated to find that combining ZnO, AlN and diamond into a layered structure would enhance the coupling coefficient and phase velocity to a significant extent. Their experimental results confirm their theoretical assumptions. Phenomenal 16 km/s phase velocity was obtained with AlN film thickness of 4.7 μm; ZnO film thickness of 1.4 μm; and spatial periodicity of 24 μm for IDTs [23].

Most piezoelectric materials (such as quartz) show phase transition temperatures below diamond deposition temperature (typically 650-1100ºC substrate temperature with 20-30 torr chamber pressure), preventing their use as a substrate for diamond growth. Langasite ($La_3Ga_5SiO_{14}$) and gallium orthophosphate ($GaPO_4$) are recently fabricated piezoelectric materials that can withstand high temperatures without being deteriorated. $GaPO_4$ phase transition temperature is 933°C, while LGS does not have phase transitions up to its melting point of 1470 °C. Both these materials are not expected to deteriorate under typical diamond CVD growth conditions. LGS is a very attractive material for SAW and BAW high-temperature applications [24-31]. It has been experimentally verified that the expected loss of piezoelectricity for quartz in between 570 and 580◦C is due to the α-β transition. The results obtained qualified the LGS crystals for high-temperature SAW gas sensors applications. Nanocrystalline diamond films have been reported to grow over LGS substrates by microwave plasma CVD [32]. Initial growth protocol and process parameters usually employed for silicon substrates were investigated but cracking and delamination of the films from the langasite substrates was then observed. To improve the adhesion property, SiO_2 was magnetron sputtered on top of an electrode of a langasite thickness-shear mode resonator. This layer was then seeded with diamond nanoparticle aqueous slurry. Nanocrystalline diamond was then grown by microwave enhanced CVD. Another method of improving adhesion was to use Argon gas for nanocrystalline diamond growth along with substrate scratching with DND slurry [33]. The nanocrystalline diamond was grown on top of a SiO_2 buffer layer [32] and thus was electrically isolated from the top contact. An alternative design was used where the interlayer supporting diamond growth was switched to tungsten. Tungsten is a well-known substrate for diamond growth. Boron-doped nanocrystalline diamond was grown on

top of 100 nm thick tungsten layer. This device has much lower loading due to thinner metal interlayer and no SiO_2buffer layer, and also there is electrochemical access to the diamond layer. Researchers at Hasselt University, Belgium and IMEC, Belgium (Oliver A Williams and co-researchers) have tried to exploit the high phase transition temperature (933^oC) of gallium orthophosphate for depositing diamond on top of it by CVD, but due to the chemical instability of $GaPO_4$, it was found that the bare $GaPO_4$ were substantially etched in the microwave plasma and no significant diamond growth occurred. To circumvent this, SiO_2 buffer layer was used. So with interlayer, $GaPO_4$could withstand the temperature of the diamond growth plasma. The phase response when plotted against frequency for this resonator, both before and after diamond growth, it was found that the response had changed very little by exposure to the harsh diamond growth environment.

Diamond films are an excellent material for protection and passivation, avoiding degradation of devices with time, and protecting the devices against hostile operating conditions. The phase velocity in diamond is higher than in common piezoelectric materials (e.g. 14mm/μs for longitudinal waves against 8.9mm/μs in SiO_2), so faster devices can be fabricated. Diamond's high heat conductivity also increases the devices power handling capability. Traditional fabrication procedures involve the deposition of the piezoelectric material on a thick diamond film [34-38]. The approach followed in this work is the opposite: the diamond film will be deposited directly on the piezoelectric material surface, simplifying the fabrication procedure to its maximum extent. Special care will be taken in the nucleation procedure [39]. Since diamond CVD takes place at substrate temperatures higher than 500ºC, the piezoelectric substrates will be LGS. LGS is expected to survive the diamond growth conditions, in particular, the exposure of the atomic hydrogen, and do not suffer any phase transition up to typical diamond deposition temperatures. This work has two-fold significances, a) finding encapsulation material for SAW devices under harsh environment and b) increasing the operating frequency of SAW device by using piezo/diamond layered structures.

2. MATERIALS & METHODS

Langasite substrates (purchased from M/s The Roditi International Corporation, UK) [40] were chosen for depositing diamond films by microwave plasma CVD. Silicon substrates (p-type, 0.5 mm thick, one side polished, 1-20 Ω-cm) were processed with each langasite substrate to compare their results. 50% of the substrates were kept inside CVD chamber (ARDIS-100, 2.45 GHz, 5 kW) under low temperature (500^oC)diamond growth conditions [41]for facilitating the formation of the thin carbonaceous layer, before undertaking conventional ultrasonic seeding (US) procedure with detonation nanodiamonds [42]. So the LGS samples were divided into two groups: one set of samples with low-temperature pre-treatment (LTPT) and the other set without any pre-treatment (NOPT). All the samples were then kept under CVD growth environment (GC) of 700^oC, 60 Torr pressure, 2.5 kW microwave power, 500 sccm of hydrogen and 20 sccm of methane flow rates. Together this process can be termed as modified novel nucleation process (NNP) [43]. Roughness plays a very important role in enhancing the diamond nucleation and growth [44,45]. To study the effect of roughness of the substrate on the diamond deposition, it was further decided to keep the samples inside the CVD chamber, either polish or rough side, facing up the microwave plasma environment. The experimental procedures have been schematically described in Figure **1**.

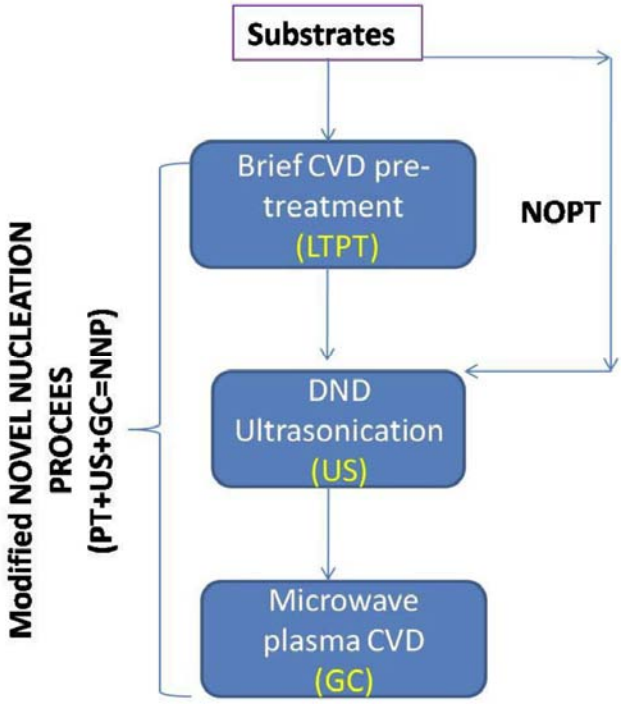

Figure 1: Schematic representation of the CVD experimental procedures.

After 2 hours of diamond growth (GC), the samples were taken out and later they were characterised by X-ray diffractometer (XRD, PW 1710, Philips Research Laboratory, Eindhoven, The Netherlands), field emission scanning electron microscopy (FESEM, LEO 430i Steroscan, UK), X-ray photoelectron spectroscopy (XPS, PHI 5000 Versaprobe II, UL-VAC PHI, USA) and, Raman spectroscopy (STR500, Cornes Technologies, formerly known as Seki Technotron) for their physical property evaluation.

3. RESULTS AND DISCUSSION

3.1. Raman Spectroscopy

Crystalline diamond gives a sharp Raman peak at 1332.28 cm^{-1} with up-shift or downshifts of the Raman line in accordance with the presence of compressive or tensile stress inside the crystal respectively [46]. The line width of the peak becomes broader with a decrease in crystal size.

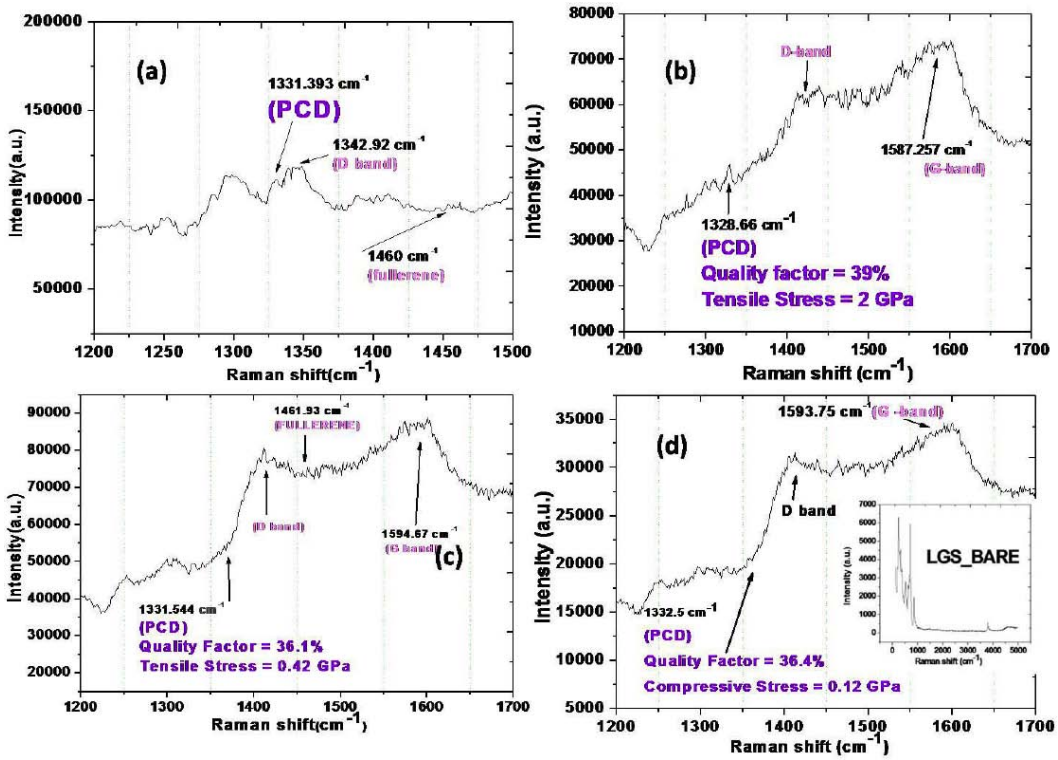

Figure 2: Raman spectroscopy of polycrystalline diamond deposited on the substrates (**a**) Si, (**b**) unpolished side of LGS with low-temperature pretreatment (LTPT), (**c**) unpolished side of LGS without substrate pretreatment (NOPT) and, (**d**) polished side of LGS without substrate pretreatment (NOPT).

On the other hand, graphite produces Raman peaks at 1350cm^{-1} and 1582 cm^{-1} respectively. Shifting of graphite theoretical peak occurs due to crystalline interaction with graphene layers and broadening of their peaks is due to the conversion of sp2 carbon into non-crystalline sp2 carbon. In Raman spectra of PCD material, the presence of a band at 1350 cm^{-1}(D) or 1580 cm^{-1}(G) signifies the graphitic impurities of the films, although the Raman signals are much more sensitive to graphite than a diamond phase. Other than diamond and graphite, there are other forms of carbon which produce Raman peaks at many different positions, like nanocrystalline diamond or surface defect modes in diamond give a band or shoulder at 1620cm^{-1}; amorphous sp3 bonded carbon gives a broad peak at 500cm^{-1}; a sharp peak at 1462cm^{-1} is for fullerene; 2700 cm^{-1}Raman signal is called G´ or 2D band and is due to graphene layers; 1350cm^{-1} graphite band is an indication of disorder in graphite crystal which otherwise produces sharp single crystal peak at 1575cm^{-1}; activated charcoal or carbon black gives Raman peak at 1355cm^{-1}; sometimes microcrystalline diamond (MCD) gives 1150cm^{-1} peak due to nanocrystalline phases with trans-polyacetylene peak at 1480 cm^{-1} [47-52]. Figure **2** depicts the Raman signals obtained from different films deposited on different substrates in this work. Figure **2a** is the signal from PCD film on a silicon substrate. It can be seen that PCD Raman peak at 1331.39 cm^{-1} is present with some downshift, due to tensile stress in the film. But disordered graphite band at 1342.92 cm^{-1} is interfering with the diamond signal in Figure **2a**. There are many other unidentified peaks in Figure **2a**, out of which peak at 1460 cm^{-1} is attributed due to the presence of fullerene. Figure **2b** is the Raman signals from the diamond coating deposited on the unpolished side of the LGS substrate, which was pre-treated in low temperature of 500^{o}C before ultrasonic seeding by detonation nanodiamond. Pre-treatment under the influence of microwave plasma PCD recipe would create a thin carbonaceous layer on top of LGS substrate. The identical temperature of 700^{o}C used for diamond deposition could not be applied during PT, as it was observed that there was degradation of the LGS substrate at a higher processing temperature of plasma [32]. Now, LTPT treatment of LGS would facilitate diamond phase formation during the actual run, which is evidenced by the Raman signal at 1328.66cm^{-1} in Figure **2b**. It is to be noted the LTPT treatment also co-deposited disordered graphite (D-band) and graphitic G band positions. Figure **2b** also has many unidentified peaks, which can also be due to noise in data collection. But, it is the practice to calibrate the instrument and also to take background spectra before each Raman measurement. The important thing to compare between the Figure **2a** and **2b** is that both are the Raman signals from diamond films but one is grown on a commonly used silicon substrate and the other one is the special substrate LGS used in the present paper. Now, if one looks at the y-axis then one would imagine that the intensities of the diamond signals are as high as 5000 a.u. for the LGS substrate, which is higher than the corresponding Raman signal for the diamond film grown on the silicon substrate. Now Figure **2c** and **2d** are the Raman signals for the film deposited on the

unpolished and polished sides of the LGS substrate without any PT respectively. We could see those diamond peak signatures are present along with graphitic G band and D band, as found in Figure **2b**. PCDs on the LGS substrates without pre-treatment have less stress with smaller downshift/upshift of the Raman peak compare to LTPT substrate. The quality factor (intensity ratio of the diamond (I_d) to graphite-like carbon (I_{glc}) peaks) is best for Figure **2b**, whereas, the stress is least for Figure **2d**. Again, it is to be noted that the intensities for the diamond signal are very small (Figures **2c** and **2d**) compared to the graphite or non-diamond signals, but high enough for not being a noise. It is a well-known fact that the graphite carbon is much more sensitive to Raman scattering than sp3 bonded carbons present in diamond material. The sudden jump in intensity while acquiring the Raman signals in approaching the typical 1332 cm^{-1} diamond signature peak position is certainly not due to noise levels in Figures **2c** and **2d**. The films deposited on LGS have very high-quality factors, which is due to the fact that Raman peak intensities are significant in comparison to the graphite signals.The films deposited on the smooth side of the LGS substrate has the least amount of stress and it is compressive in nature, whereas, the rough side of the same NOPT substrate gives tensile stress but not as much as the rough side of the LGS substrate with LTPT. It may be that prior deposition of sp3 rich carbon film introduces more defect in the growing film than film deposited without PT. Figure **2** has many unidentified peaks correspond to other forms of amorphous and nanocrystalline carbon which could not be labelled in the present work. All the films deposited on the LGS have similar spectral features (Figures **2b-d**). Bare LGS substrate (inset of Figure **2d**) was also studied with Raman laser and was found to contain no peak in the range where carbon gives a signal to 514.5 nm laser excitation. It is inferred from the Raman data that the roughness of the substrate changes the nature of the diamond film internal stress from compressive to tensile, whereas, this inherent tensile stress in the film deposited on the rough side is further enhanced with low-temperature pre-treatment (LTPT) of the LGS substrate. Moreover, the diamond film quality does not get much altered with the change in the substrate roughness but with the substrate pre-treatment.

3.2. XRD and XPS

Diamond cubic crystals give characteristic (111), (220), (311) and (400) plane diffraction peaks at about 44°, 75°, 91° and 119° 2θ values according to JCPDS file no. 6-0675 [53]. But when we carried out routine X-ray diffraction scan on the diamond-coated Si and LGS substrates, it was observed that the peaks were coming at 2θ values which are not usual. It was first tried to manually fit the peak positions with maximum possible intensity from Joint Committee for Powder Diffraction Standard (JCPDS) files, but later on, "X'pert Pro

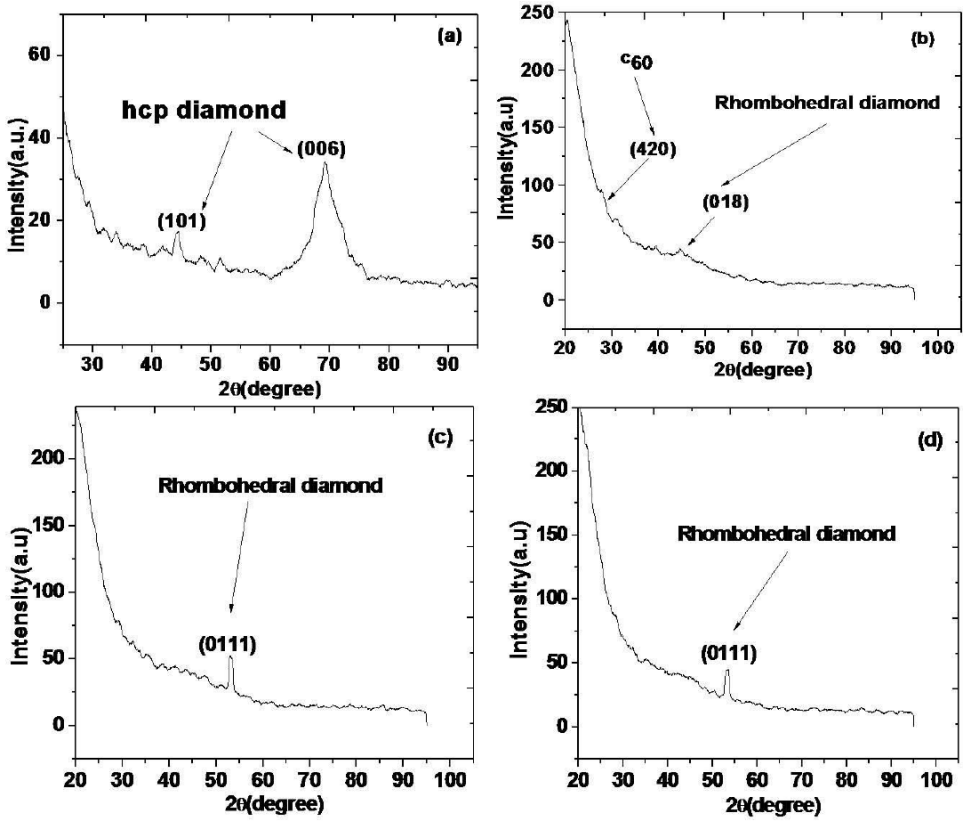

Figure 3: XRD micrographs of polycrystalline diamond deposited on the substrates (**a**) Si, (**b**) unpolished side of LGS with low-temperature pretreatment (LTPT), (**c**) unpolished side of LGS without substrate pretreatment (NOPT) and, (**d**) polished side of LGS without substrate pretreatment (NOPT).

software" (High Score Plus 3.0e, 2012version) was also used to fit the data automatically. Diamond-coated silicon wafers experimentally showed two peaks at 44.09° and 69.4° with 2.05Å and 1.36 Å d-spacing respectively. These two values were best manually fitted with JCPDS file numbers 79-1468 and 79-1470 for hexagonal primitive diamond lattice for diffraction planes of (002) and (107) respectively. But when the same peaks were also fitted with automated software X'pert Pro, then JCPDS file no. 79-1469 was found to be appropriately matched with corresponding reflections from (101) and (006) of hcp diamond lattice as shown in Figure **3a**. Similarly, the diamond-coated rough side of the LGS substrate with LTPT also produced X-ray peak at 44.89° 2θ value with 2.02Å d-spacing but one additional peak appeared at 28.12° with 3.17Å d-spacing. So the diamond material deposited on LGS must have been different from the diamond deposited on Si. It was manually found to fit best with JCPDS file numbers 79-1470 and 79-1471 for (004) and (103) reflection planes of a hexagonal primitive diamond. But when the same data were fed into X'pert pro software, the best match came up with JCPDS file no. 79-1473 for a rhombohedral diamond with reflection plane of (018) at 44.89°, and to our surprise the other peak at 28.12° was best fitted with (420) reflection for C_{60} fullerene, as shown in Figure **3b**. Raman signals from films on different substrates also indicated the presence of fullerene in the deposited films (Figures **2a** and **2c**). The diamond coatings on LGS substrates without pretreatment (NOPT) also showed PCD Raman peaks, both from the rough and polished sides. Now, both of them also showed crystalline X-ray diffraction peaks; rough side peak at 53.31° with d-spacing of 1.72Å and polished side peak at 53.2° with d-spacing of 1.72Å. Manually this peak could be best fitted with (103) reflection plane of hexagonal primitive diamond lattice from 79-1469 JCPDS file. On the other hand "X'pert pro software" matched this peak with JCPDS file no. 79-1472 with the rhombohedral diamond plane (0111) as shown in Figures **3c** and **3d**. It is found that none of the X-ray diffraction peaks could be matched with conventional diamond cubic structure. It is perhaps a new diamond phase formed on the langasite substrate. But the film deposited on Si was also found not to be cubic, but hexagonal. It may be so that since Si was kept alongside the LGS substrate during CVD growth of diamond, the plasma chemistry altered the diamond growth process in the present experiments.

Now to know the elements present on the diamond-coated LGS substrate, further X-ray photoelectron spectroscopy was carried out with wide-area surface scan only. The XPS data revealed that the substrate surface is coated with carbon. 284.4 eV is the actual C1s peak position, which has been upshifted by 0.17 eV in the present case (Figure **4a**). Interestingly, the diamond surface was found to be oxygenated (Figure **4c**), as found in the authors' previous work [54]. The upshift of C1s peak indicates that the films are of better varieties. There was no additional XPS signal from the base $La_3Ga_5SiO_{14}$ as shown in Figure **4b**. Absence of any signal from Si (Figure **4d**) negates the suspicion that the surface may have some silicon carbide phase.

3.3. SEM and EDAX

Figure **5** is the scanning electron microscope images of the polycrystalline diamond films deposited on different substrates. It is observed that the grains are somewhat agglomerated on Si, with an average grain size of 175 nm (Figure **5a**). The similar size of about 187 nm was also observed for diamond grains deposited on the rough side of the LGS substrate without prior substrate treatment under microwave plasma growth environment (Figure **5c**). But when the diamond films were grown on the smooth polished side of similarly not pre-treated LGS substrate, it was found that the grains are having a somewhat smaller size of 145 nm (Figure **5d**). The average grain size difference between the diamond grains on rough and smooth sides of LGS with NOPT is due to their difference in surface roughness. As it is known that the rough surface enhances nucleation and growth of the diamond film [44], it can be inferred that when the substrate was ultrasonically treated with detonation nanodiamond slurry before deposition, more number of grooves and pits were created, which acted as favourable high energy sites for adatoms from plasma environment to attach onto the rougher side. Moreover, the rough surface also had inherent cavities for the DND particles to get entrapped for better nucleation enhancement. This may be one reason for getting bigger diamond grains on the rough side than on the polished side. The other reason may be that since the rough surface of the LGS substrate would have more active sites for adsorption of plasma species for diamond growth than the smoother surface, and then it would have more nucleation density than a polished surface and may be responsible for resulting big diamond grains. Figures **5c** and **5d** show the effect of substrate roughness on the resulting CVD grown diamond grain size. To understand the effect of PT on the grain size, Figures **5b** and **5c** should be compared for the films deposited on similar rough sides. It can be found that higher active sites on the rough surface in conjugation with substrate pre-treatment (LTPT) have led to much bigger grain size of 823 nm, compare to about 187 nm size diamond crystals grown on the LGS substrates with NOPT as seen in the microstructure of Figure **5b**, which is very much different from the diamond grains observed on other substrates. Figure **5b** is the diamond film on the rough side of the LGS substrate but with low-temperature pre-treatment (PT) under diamond growth environment for covering the substrate with sp3 rich carbon layer before US and GC. LTPT of the substrate might have rendered special quality on the surface which resulted in elongated and curvy grains of diamond, which at the best possible metaphor can be described as a small island like structures. Lower magnification image in Figure **6a** provides a better understanding of the overall structures. There are some voids visible in between elongated curvy diamond grains, and together, they also can be viewed as an active volcano site from the top. The black holes represent the

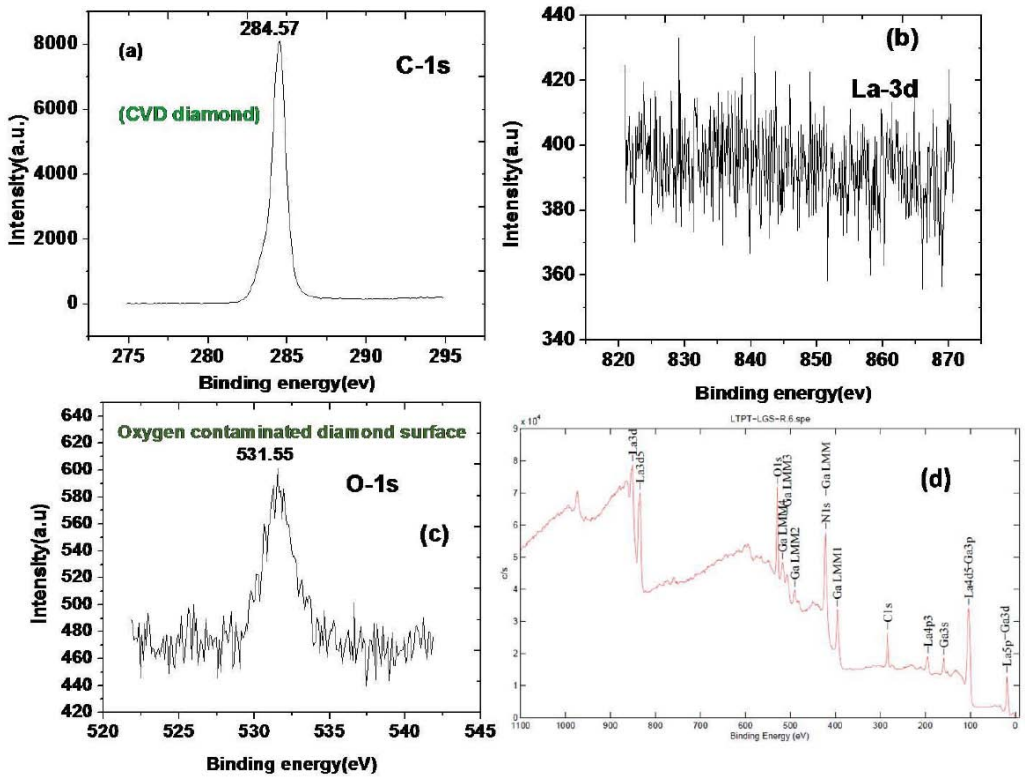

Figure 4: XPS signals of diamond-coated LGS substrate with low-temperature pre-treatment (LTPT) (**a**) C-1s, (**b**) La-3d and (**c**) O-1s, (**d**) wide surface scan on the coated rough side.

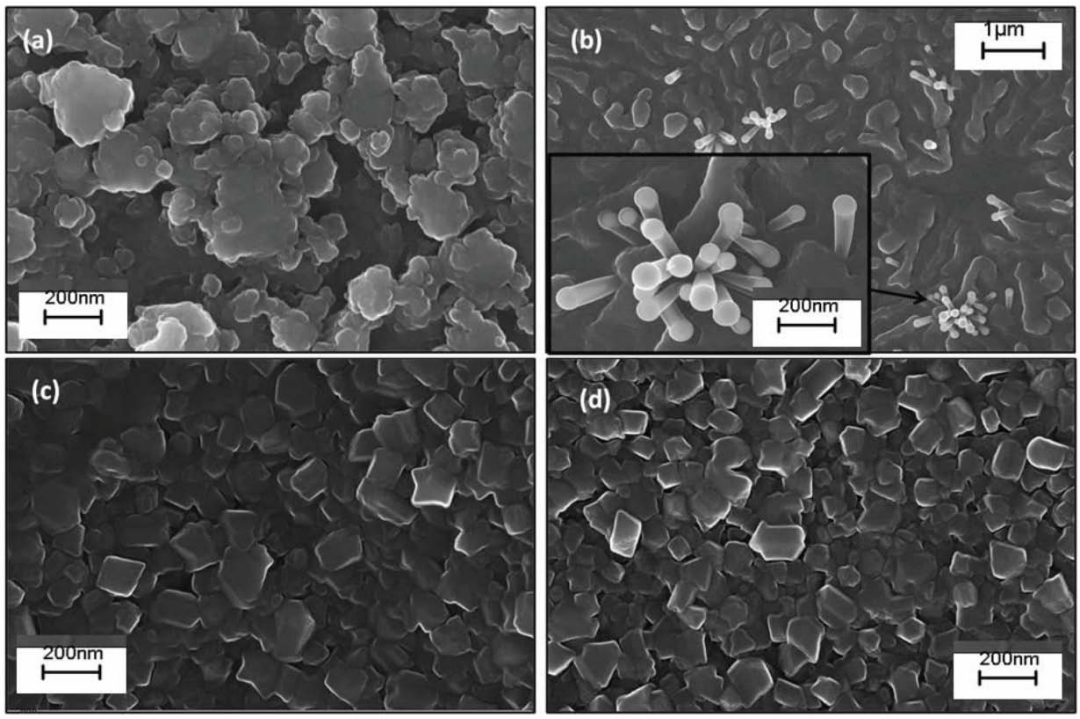

Figure 5: FESEM microstructure images of polycrystalline diamond deposited on the substrates (**a**) Si, (**b**) unpolished side of LGS with low-temperature pretreatment (LTPT), (**c**) unpolished side of LGS without substrate pretreatment (NOPT) and, (**d**) polished side of LGS without substrate pretreatment (NOPT).

mouth of eruptions and the adjacent grains can be imagined as out-flowing molten lava from inside. The metaphor of eruption can be extended to the spike-like features, as in the inset Figure **5b**, which are emanating from the underneath. Now a closer look at the successive circled regions of Figure **6** would reveal that some kind of rope-like structures is

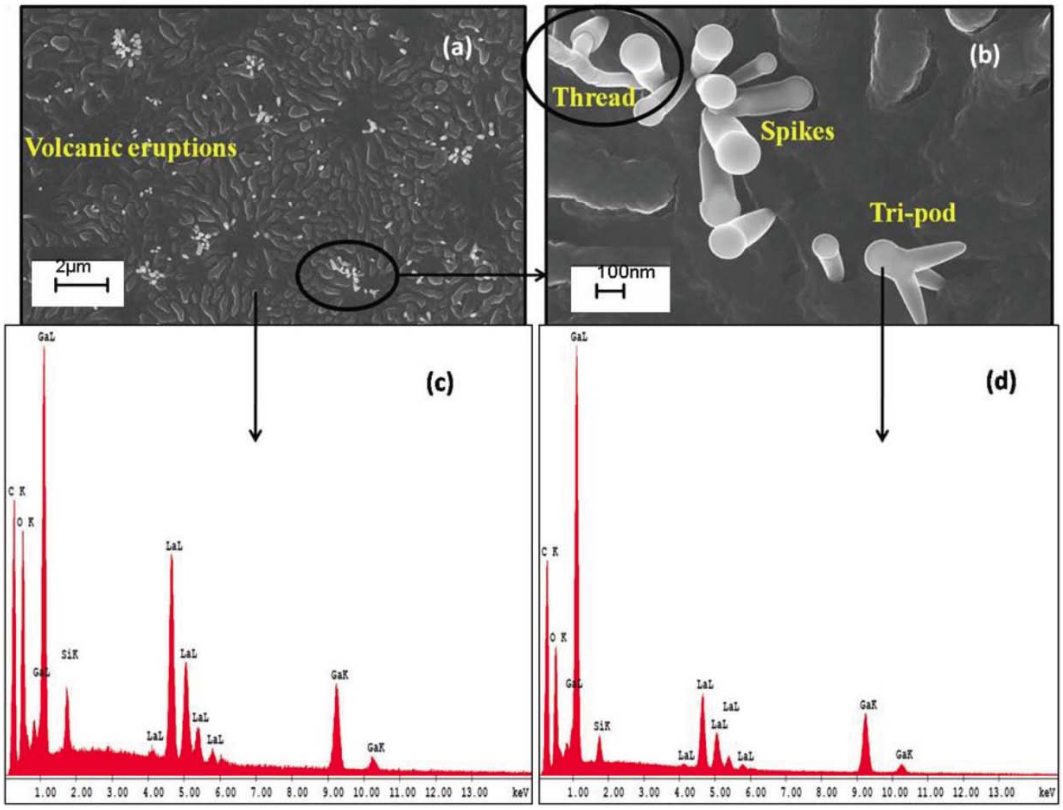

Figure 6: (**a**) Active volcano-like microstructures of PCD grown over the rough side of LGS substrates with low-temperature pretreatment, (**b**) enlarged view of the circled portion from Figure **6a**, (**c**) EDAX signals from the island like granular region and, (**d**) EDAX signal from the tripod-like region.

extruding out from the spikes. Although, the spikes are rigid in appearance but the thread that is coming out from the centre of such rod is not rigid but slacking. Additionally, some kind of tripod formation is also visible in Figure **6b**. The EDAX signals from both the elongated curvy grains and from the rod-like spikes give similar data as seen in Figure **6c** and **6d**. Both the signals are almost identical, inferring same chemical nature of such unique microstructural features throughout the surface. Now, it is important to notice that the most prominent peak is for Ga, along with the presence of low-intensity peaks for La, Si and O in Figure **6**. The base substrate is $La_3Ga_5SiO_{14}$. If we look at Figure **7b**, which is EDAX for bare LGS substrate, all the substrate elements produce prominent sharp peaks. Since carbon was coated before electron microscopy, we could also observe EDAX signal for carbon with less intensity. On the other hand, LGS substrate after CVD run produces EDAX signals with reduced intensity for the substrate elements and with enhanced intensity peak for carbon, Figures **7c** and **7d**, irrespective of their substrate roughness. Now, the carbon film has already been confirmed to consist of PCD and sp2 carbons from Raman spectroscopy, Figure **2**. But the EDAX signals from the films coated on the rough and polished sides of LGS without pre-treatment, Figures **7c** and **7d**, show carbon giving the highest intensity peak, and all other peaks from the substrate elements are much subdued. If we compare **7c** and **7d** peak intensities, although the elemental signatures are identical, but their intensities are higher for Figure **7d**. Such information throws some light on the effect of substrate roughness on the nature of the deposited films. Since the base substrate elements are giving marginally higher intensity signals for the films grown on the LGS polished side, it can be concluded that the film may be thinner, and which also had already been indicated by their smaller grain sizes in Figure **5d**. Now, comparing EDAX signals between LTPT (6c) and NOPT (7c) substrates (both unpolished), it can be seen that the substrate pretreatment (PT) does not suppress Ga and La elemental peaks much like the diamond film does for NOPT substrate. So it is evident that the substrate pre-treatment of LGS plays an important role in altering the nucleation and growth behaviour of the deposited diamond film. First, it shows unique microstructural features and secondly, the I_d/I_d+I_{glc} ratio is also found to be the highest, signifying the best quality diamond film among all the deposited PCDs. Figure **7a** also shows the EDAX signal for the film deposited on the silicon substrate, where the substrate (Si) peak is of higher intensity than carbon film (not like the LGS substrates Figures **6c** and **6d**, where the substrate signals are of lower intensity than carbon film). There is no other elemental peak present in a film deposited on Si.

4. CONCLUSIONS

Diamond was successfully deposited on $La_3Ga_5SiO_{14}$ substrates without the need of any interlayer as earlier

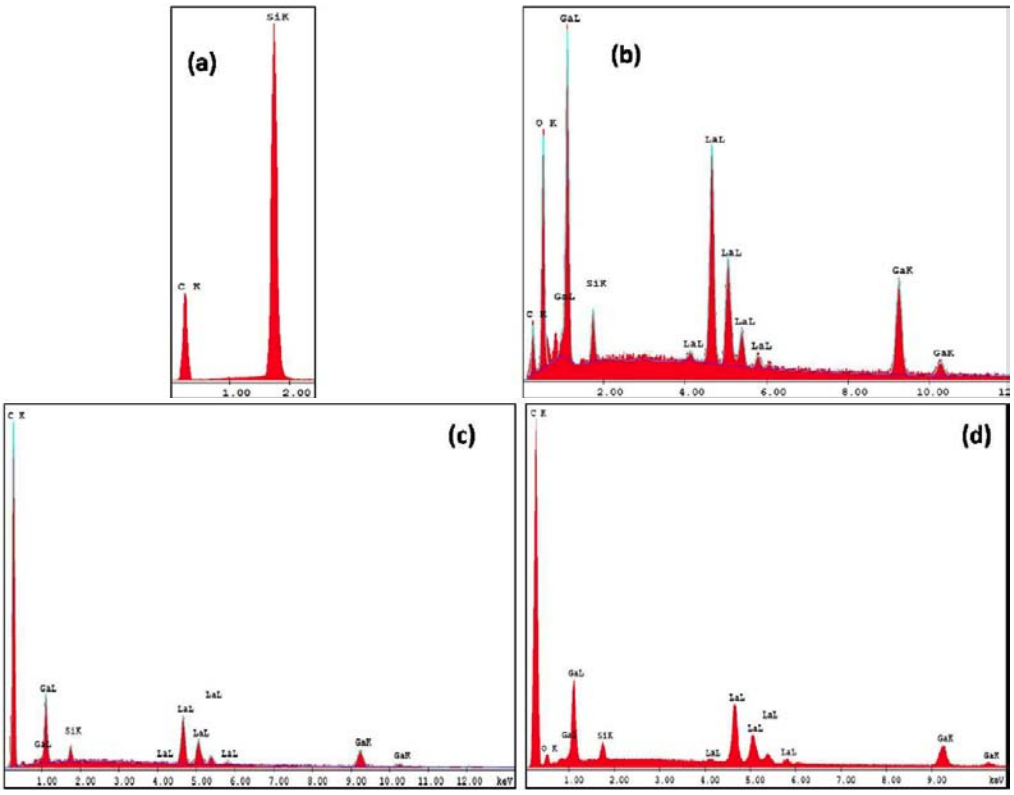

Figure 7: EDAX peaks of (**a**) diamond coated Si, (**b**) uncoated, unpolished side of LGS, (**c**) diamond coated unpolished side of LGS without substrate pretreatment (NOPT) and, (**d**) diamond coated polished side of LGS without substrate pretreatment (NOPT).

reported in the literature [32]. Neither, Ar rich plasma chemistry was used for improving the UNCD film adhesion nor W/SiO_2 buffer was added. PCD was co-deposited on the Si substrates with methane-hydrogen plasma, kept along with LGS inside the CVD chamber for comparing the results. Raman, X-ray, XPS peaks confirm the presence of diamond crystals. XRD micrographs interestingly show the presence of hcp and rhombohedral crystal structures of the deposited diamond film. LGS does not react or melt under the present CVD diamond growth conditions. Presence of thin layer of PCD suppresses the bare LGS EDAX elemental peaks. This layer may be thinner for the film grown on the polished side of the LGS substrate, as it was also found to be of finer grain sizes (145 nm). Volcanic eruption like microstructure is uniquely seen for the film on LGS with low-temperature pretreatment (LTPT). There are many spikes, tripods, rope-like elongated micro-structural features emanating out from the base substrate. But such unique micro-structures disappear for the LGS substrate without pretreatment (NOPT). Both the polished and unpolished sides of the substrate could favour diamond growth. It appears that the roughness of the substrate favours bigger diamond grains (187 nm). Moreover, the roughness changes the nature of the internal stress from compressive to tensile, while keeping the diamond film quality almost the same. This tensile stress gets exasperated (2 GPa) with substrate pre-treatment (LTPT) but with concomitant improvement in the film quality (39%). The rhombohedral diamond structure was detected for the film deposited on the LGS substrate, whereas the diamond film grown on silicon was hexagonal close pack structure. Films on LTPT substrate show different XRD peak positions (018) for rhombohedral structure than NOPT substrate, but the change in surface roughness does not alter the corresponding rhombohedral peak position (0111) for NOPT substrates. This research provides an understanding of the deposition of diamond on high-temperature piezoelectric materials. These materials can be used for the fabrication of wireless and passive devices that can be used in remote or inaccessible places. Even though the SAW technology is, by itself, a versatile and powerful technology, the coating of these devices with diamond opens the door to the application of these sensors under extremely hostile environments, under chemically or radioactive aggressive atmospheres or in places where the sensors are exposed to high wear and tear. Diamond CVD is a technique widely used for the coating of a variety of substrates for different applications; however, the deposition of diamond films on piezoelectric materials is an area that has not been explored. As such, the work and knowledge obtained during this study are expected to have a real impact on the development of a new generation of SAW-based sensors and devices with increased operational frequencies.

ACKNOWLEDGEMENTS

CSIR, India (PSC0101) and DST, India (GAP0246) financially supported CVD diamond research activity at CSIR-CGCRI. The diamond films were prepared at Diamond Materials

Laboratory, GPI-RAS, Moscow, Russia. The LGS substrates were received from the University of Aveiro, Portugal. AKM acknowledges FWO-Research Foundation Flanders for a postdoctoral fellowship.

REFERENCES

[1] Hauser R, Reind L, Biniasch J. High –temperature stability of LiNbO3 based SAW devices. IEEE Ultrasonics Symp 2003; 1: 192.

[2] Bulst W, Fischerauer G, Reind L. State of the art in wireless sensing with surface acoustic waves. IEEE Trans Ind Elect 2001; 48: 265. https://doi.org/10.1109/41.915404

[3] Ostermayer G, Pohl A, Steindl R, Seifert F. SAW sensors and correlative signal processing – a method providing multiple access capability. Proc IEEE 5th Int Symp Spread Spectrum Tech Appl 1998; 3: 902. https://doi.org/10.1109/ISSSTA.1998.722509

[4] Mukherjee D, Oliveira F, Silva R, Carreira J, Rino L, Correia M, Rotter S, Alves L, Mendes J. Diamond-SAW devices: a reverse fabrication method. Phys Stat Sol (C) 2015; 13: 53-8. https://doi.org/10.1002/pssc.201510313

[5] Jagannadham K, Lance M, Watkins T. Growth of diamond film on single crystal lithium niobate for surface acoustic wave devices. J Vac Sc Tech 2004; A22: 1105. https://doi.org/10.1116/1.1740770

[6] Jagannadham K, Watkins T, Lance M. Interfacial characterization and residual stress analysis in diamond films on LiNbO3. J Vac Sc Tech 2006; A 24: 2105. https://doi.org/10.1116/1.2356479

[7] Thiele J, Cunha M. High temperature SAW gas sensor on langasite. Proc IEEE Sensors 2003; 2: 769. https://doi.org/10.1109/ICSENS.2003.1279045

[8] Seh H, Tuller H, Fritze H. Langasite for high-temperature acoustic wave gas sensors. Sensors and Actuators B 2003; 93: 169-74. https://doi.org/10.1016/S0925-4005(03)00189-8

[9] Thiele J, Cunha M. High temperature LGS SAW gas sensor. Sensors and Actuators B 2006; 113: 816-22. https://doi.org/10.1016/j.snb.2005.03.071

[10] Tortissier G, Blanc L, Tetelin A, Lachaud L, Benoit M, Conedera V. Langasite based surface acoustic wave sensors for high temperature chemical detection in harsh environment. Proc Chemist 2009; 1: 963-66. https://doi.org/10.1016/j.proche.2009.07.240

[11] Rotter S, Madaleno J. Diamond CVD by a combined plasma pretreatment and seeding procedure. J Chem Vap Dep 2009; 15: 209-16. https://doi.org/10.1002/cvde.200806745

[12] Shenderova O, Hens S, McGuire G. Seeding slurries based on detonation nanodiamond in DMSO. Diamond Relat Mat 2010; 19: 260-67. https://doi.org/10.1016/j.diamond.2009.10.008

[13] Bi B, Huang W, Asmussen J, Golding B. Surface acoustic waves on nanocrystalline diamond. Diamond Relat Mat 2002; 11: 677-80. https://doi.org/10.1016/S0925-9635(01)00621-5

[14] Kulha P, Kromka A, Babchenko O, Vanecek M, Husak M, Williams O, Haenen K. Nanocrystalline diamond piezoresistive sensor. Vacuum 2010, 84: 53-6. https://doi.org/10.1016/j.vacuum.2009.04.023

[15] Yamamoto A, Sutsumoto T. Nanocrystalline diamond piezoresistive sensor. Diamond Relat Mat 2004; 13: 863-66. https://doi.org/10.1016/j.diamond.2003.12.017

[16] Yamamoto A, Nawachi N, Tsutsumoto T, Terayama A. Pressure sensor using p-type polycrystalline diamond piezoresistors. Diamond Relat Mat 2005; 14: 657-60. https://doi.org/10.1016/j.diamond.2004.09.001

[17] Sahli S, Aslam D. Ultra-high sensitivity intra-grain poly-diamond piezoresistors. Sensors and Actuators A 1998; 71: 193-97. https://doi.org/10.1016/S0924-4247(98)00181-2

[18] Tibrewala A, Peiner E, Bandor R, Biehl S, Lüthj H. Longitudinal and transversal piezoresistive effect in hydrogenated amorphous carbon films. Thin Solid Films 2007; 515: 8028-33. https://doi.org/10.1016/j.tsf.2007.03.046

[19] Shikata S, Nakahata H. Diamond surface acoustic wave device, Chapter 8. Semicond Semimet 2004; 77: 339-58. https://doi.org/10.1016/S0080-8784(04)80020-6

[20] Chen J, Zeng F, Li D, Niu J, Pan F. Deposition of high-quality zinc oxide thin films on diamond substrates for high-frequency surface acoustic wave filter applications. Thin Solid Films 2005; 485: 257-61. https://doi.org/10.1016/j.tsf.2005.04.028

[21] Benedic F, Assouar M, Mohasseb F, Elmazria O, Alnot P, Gicquel A. Surface acoustic wave devices based on nanocrystalline diamond and aluminium nitride. Diamond Relat Mat 2004; 13: 347-53. https://doi.org/10.1016/j.diamond.2003.10.020

[22] Lamara T, Belmahi M, Elmazria O, LeBrizoual L, Bougdira J, Remy M, Alnot P. Freestanding CVD diamond elaborated by pulsed-microwave-plasma for ZnO/diamond SAW devices. Diamond Relat Mat 2004; 13: 581-84. https://doi.org/10.1016/j.diamond.2003.10.075

[23] Hakiki M, Elmazria O, Assouar M, Mortet V, Brizouaa L, Vanecek M, Alnot P. ZnO/AlN/diamond layered structure for SAW devices combining high velocity and high electromechanical coupling coefficient. Diamond Relat Mat 2005; 14: 1175-78. https://doi.org/10.1016/j.diamond.2005.01.002

[24] Mill B, Pisarevsky Y. Langasite-type materials from discovery to present state. Proc of the Annual IEEE Int Freq Control Symp 2000; 133-40.

[25] Kosinski J. New piezoelectric substrates for SAW devices. Adv SAW Tech Syst Appl 2001; 20: 151-202. https://doi.org/10.1142/9789812811561_0003

[26] Cunha M, Fagundes S. Investigation on recent quartz like materials for SAW applications. IEEE Tran Ultrasonics, Ferroelectrics, and Frequency Control 1999; 46: 1583-90. https://doi.org/10.1109/58.808884

[27] Krempl P, Reiter C, Wallnofer W, Neubig J. Temperature sensors based on GaPO4. Proc IEEE Ultrasonics Symp 2002; 1: 949-52.

[28] Honal M, Fachberger R, Holzheu T, Riha E, Born E, Pongratz P, Bausewein A. Langasite surface acoustic wave sensors for high temperatures. Proc Ann IEEE Int Freq Control Symp 2000; 113-8.

[29] Fritze H, Tuller H, Borchardt G, Fukuda T. High temperature properties of langasite. Proc Mat Res Soc Symp 2000; 604: 65-70. https://doi.org/10.1557/PROC-604-65

[30] Thiele J, Cunha M. High temperature surface acoustic wave devices: fabrication and characterization. Elect Lett 2003; 39: 818-9. https://doi.org/10.1049/el:20030511

[31] Wang S, Harada J, Uda S. A wireless surface acoustic wave temperature sensor using langasite as substrate material for high temperature applications. Jap J Appl Phys 2003; 42: 6124-27. https://doi.org/10.1143/JJAP.42.6124

[32] Williams O, Mortet V, Daenen M, Haenen K. Nanocrystalline diamond enhanced thickness shear mode resonator. Appl Phys Lett 2007; 90: 063514. https://doi.org/10.1063/1.2471649

[33] Hakiki M, Elmazria O, Bénédic F, Nicolay P, Monéger D, Azouani R. Diamond film on Langasite substrate for surface acoustic wave devices operating in high frequency and high temperature. Diamond Relat Mat 2007; 16: 966-9. https://doi.org/10.1016/j.diamond.2006.09.002

[34] Shikata S, Nakahata H, Higaki K, Fuji S, Kitabayashi H, Tanabe K, Seki Y. SAW device application of diamond. 18th IEEE International CPMT 1995; 379-82.

[35] Lee Y, Lin S, Buck V, Kunze R, Schmidt H, Lin C, Fang W, I.N. Lin I. Surface acoustic wave properties of natural smooth ultra-nanocrystalline diamond characterized by laser-induced SAW pulse technique. Diamond Relat Mat 2008; 17: 446-50. https://doi.org/10.1016/j.diamond.2007.08.025

[36] Bénédic F, Assouar M, Kirsch P, Monéger D, Brinza O, Elmazria O, Alnot P, Gicquel A. Very high frequency SAW devices based on nano-crystalline diamond and aluminum nitride layered structure achieved using e-beam lithography. Diamond Relat Mat 2008; 17: 804-8. https://doi.org/10.1016/j.diamond.2007.10.015

[37] Benetti M, Cannatà D, Pietrantonio F, Verona E. Growth of AlN Piezoelectric Film on Diamond for High-Frequency Surface Acoustic Wave Devices. IEEE Trans on Ultrasonics, Ferroelectrics and Frequency Control 2005; 52: 1806-11. https://doi.org/10.1109/TUFFC.2005.1561635

[38] Park S, Kim J, Park S, Son M, Kim Y, Abe T, Takagi T. Study on the Surface Wave Propagation in the Diamond Coated Silicon. IEEE Ultrasonics Symp 2007; 2291-94. https://doi.org/10.1109/ULTSYM.2007.576

[39] Rotter S, Madaleno J. Diamond CVD by a combined plasma pretreatment and seeding procedure. J Chem Vap Dep 2009; 15: 209-16. https://doi.org/10.1002/cvde.200806745

[40] http://www.roditi.com/SingleCrystal/Langasite/Langasite-Wafers-Boules.html, last accessed on 19th December, 2019.

[41] Parkhomenko M, Kalenov D, Fedoseev N, Eremin S, Ralchenko V, Bolshakov A, Ashkinazi E, Popovich A, Balla V, Mallik A. Measurement of the Complex Permittivity of Polycrystalline Diamond by the Resonator Method in the Millimeter Range. Phys Wave Phen 2015; 23: 1-6. https://doi.org/10.3103/S1541308X15030073

[42] Mallik A, Mendes J, Rotter S, Bysakh S. Detonation nanodiamond seeding technique for nucleation enhancement of CVD diamond – some experimental insights. Adv Ceramic Sc Engg 2014; 3: 36-45. https://doi.org/10.14355/acse.2014.03.005

[43] Mallik A, Bysakh S, Bhar R, Rotter S, Mendes J. Effect of seed size, suspension recycling and substrate pre-treatment on the CVD growth of diamond coatings. O J Appl Sc 2015; 5: 747-63. https://doi.org/10.4236/ojapps.2015.512071

[44] Mallik A, Binu S, Satapathy L, Narayana C, Seikh M, Shivashankar S, Biswas S. Effect of substrate roughness on growth of diamond by hot filament CVD. Bull Mater Sci 2010; 33: 251-5. https://doi.org/10.1007/s12034-010-0039-3

[45] Mallik A, Shivashankar S, Biswas S. High Vacuum Tribology of Polycrystalline Diamond Coatings. Sadhana 2009; 34: 811-21. https://doi.org/10.1007/s12046-009-0047-4

[46] Mallik A, Bysakh S, Sreemany M, Roy S, Ghosh J, Roy S, Mendes J, Gracio J, Datta S. Property mapping of polycrystalline diamond coatings over large area. J Adv Ceramics 2014; 3: 56-70. https://doi.org/10.1007/s40145-014-0093-1

[47] Chu P, Li L. Characterization of amorphous and nanocrystalline carbon films. Mat Chem Phys 2006; 96: 253-77. https://doi.org/10.1016/j.matchemphys.2005.07.048

[48] Filik J. Raman spectroscopy: a simple, non-destructive way to characterize diamond and diamond-like-materials. Spectroscopy Europe 2005; 17: 10-17.

[49] Shroder R, Nemanich R, Glass J. Analysis of the composite structures in diamond thin films by Raman spectroscopy. Phys Rev B 1990; 41: 3738-45. https://doi.org/10.1103/PhysRevB.41.3738

[50] May P, Ludlow W, Hannaway M, Heard P, Smith J, Rosser K. Raman and conductivity studies of boron-doped microcrystalline diamond, facetted nanocrystalline diamond and cauliflower diamond films. Diamond Relat Mat 2008; 17: 105-17. https://doi.org/10.1016/j.diamond.2007.11.005

[51] Hodkiewicz J. Characterizing Carbon Materials with Raman Spectroscopy. Thermo Fisher Scientific, Application Note 2010; 51901: 1-5.

[52] Ferrari A, Robertson J. Raman spectroscopy of amorphous, nanostructured, diamond-like carbon, and nanodiamond. Phil Trans R Soc Lond A 2004; 362: 2477-512. https://doi.org/10.1098/rsta.2004.1452

[53] Mallik A, Bysakh S, Pal K, Dandapat N, Guha B, Datta S, Basu D. Large area deposition of polycrystalline diamond coatings by microwave plasma CVD. Tran In. Ceramic Soc 2013; 72: 225-32. https://doi.org/10.1080/0371750X.2013.870768

[54] Mallik A, Dandapat N, Chakraborty S, Ghosh J, Unnikrishnan M, Balla V. Characterisations of microwave plasma CVD grown polycrystalline diamond (PCD) coatings for advanced technological applications. J Proc Appl Ceramics 2014; 8: 69-80. https://doi.org/10.2298/PAC1402069M